

Amyloidogenic light chains impair plasma cell survival

Marjorie Pick,¹ Eyal Lebel,¹ Sharona Elgavish,² Hadar Benyamini,² Yuval Nevo,² Rachel Hertz,³ Jacob Bar-Tana,³ Paola Rognoni,⁴ Giampaolo Merlini⁴ and Moshe E. Gatt¹

¹Department of Hematology, Hadassah Medical Center, Faculty of Medicine, Hebrew University of Jerusalem, Jerusalem, Israel; ²Info-CORE, I-CORE Bioinformatics Unit of the Hebrew University of Jerusalem, Jerusalem, Israel; ³School of Public Health, Hebrew University of Jerusalem, Jerusalem, Israel and ⁴Amyloidosis Research and Treatment Center, Fondazione IRCCS Policlinico San Matteo and University of Pavia, Pavia, Italy.

Correspondence: M. Pick
marjorie@cc.huji.ac.il

Received: November 29, 2022.

Accepted: June 20, 2023.

Early view: June 29, 2023.

<https://doi.org/10.3324/haematol.2022.282484>

©2023 Ferrata Storti Foundation

Published under a CC BY-NC license



Abstract

Systemic light chain amyloidosis (AL) is a clonal plasma cell disorder characterized by the deposition of misfolded immunoglobulin light chains (LC) as insoluble fibrils in organs. The lack of suitable models has hindered the investigation of the disease mechanisms. Our aim was to establish AL LC-producing plasma cell lines and use them to investigate the biology of the amyloidogenic clone. We used lentiviral vectors to generate cell lines expressing LC from patients suffering from AL amyloidosis. The AL LC-producing cell lines showed a significant decrease in proliferation, cell cycle arrest, and an increase in apoptosis and autophagy as compared with the multiple myeloma LC-producing cells. According to the results of RNA sequencing the AL LC-producing lines showed higher mitochondrial oxidative stress, and decreased activity of the Myc and cholesterol pathways. The neoplastic behavior of plasma cells is altered by the constitutive expression of amyloidogenic LC causing intracellular toxicity. This observation may explain the disparity in the malignant behavior of the amyloid clone compared to the myeloma clone. These findings should enable future *in vitro* studies and help delineate the unique cellular pathways of AL, thus expediting the development of specific treatments for patients with this disorder.

Introduction

Systemic light chain amyloidosis (AL) is a rare monoclonal plasma cell (PC) disorder characterized by the systemic deposition of misfolded immunoglobulin light chains (LC) as insoluble fibrils in organs.¹ Without specific therapies patients who present with amyloidogenic LC that target vital organs will ultimately die.² Furthermore, AL amyloidosis may be found in 10% of patients with multiple myeloma, in whom it confers a worse prognosis.³⁻⁶ Unlike in multiple myeloma (MM), in which the clinical picture is dominated by the hyper-proliferative MM clone, in AL severe organ dysfunction is usually caused by a small PC clone producing the amyloidogenic LC.⁷

Treatment approaches to AL are derived from MM protocols and aim at suppressing the clone with chemotherapy and novel PC targeted agents.^{8,9} Lessons learned in the clinic reveal that reducing the concentration of the circulating amyloidogenic free LC improves cardiac function and prolongs survival.^{10,11} This indicates that it is not solely the deposition of the mass of the amyloid in the tissues which causes organ injury^{1,12,13} and that toxicity of the LC

is a fundamental contributor.⁷ In AL, the PC clones are usually small (median 10% of bone marrow cells) and, interestingly, the free LC levels in AL may be 10 logs lower than in MM irrespective of serious organ damage.

Amyloid LC precursors are likely to mediate cellular toxicity through a mechanism that causes oxidative stress and activates the apoptotic pathway.^{1,14} Much research has been performed to determine the molecular factors that make a particular LC protein amyloidogenic, and to elucidate the mechanism of amyloid fibril formation and even to characterize the amyloid formation *in vitro*, with some success at unveiling the process.^{1,12,14,15}

To date, there are only two characterized amyloidogenic cell lines, which were produced from the same patient.¹⁶ Their limits are the lack of an analogous control non-amyloidogenic line, and their ability to produce only one type of LC.

Both MM and AL originate from a neoplastic PC clone; however, AL has an attenuated proliferative physiology and different clinical behavior. Several lines of evidence indicate that the amyloidogenic clone is at the crossroads between monoclonal gammopathy of undetermined sig-

nificance and MM, with less mutation burden,¹⁷ more stable genetic status,¹⁸ and lower intraclonal heterogeneity¹⁹ than MM. Previous reports indicate that amyloid LC determine endoplasmic reticulum oxidative stress in the PC that produce them, sensitizing the clone to the action of proteasome inhibitors and thus providing a molecular basis for the exquisite sensitivity to these agents observed in the clinic.²⁰ The same mechanism has been shown in PC producing LC that also aggregate causing LC deposition disease.²¹

Here we report the establishment of a model to study the molecular mechanisms underlying amyloid LC proteotoxicity. We used lentiviral vectors that contain cloned LC sequences from patients with AL amyloidosis with cardiac or renal involvement and from patients with MM to enable stable expression of LC in MM cell lines. The purpose of our study was to investigate the effects of amyloid LC on PC proliferation and metabolism, two key aspects that were not explored in the previous two studies that focused on endoplasmic reticulum stress and protein degradation pathways.^{20,21}

Methods

Cell lines

The cell lines used were: KMS11 and NCI-H929 (MM cell lines), HL60 (an acute promyelocytic leukemia cell line), 721.221 (an HLA-negative B-cell line) and 293T or HEK293T (a human embryonic kidney cell line that expresses a mutant version of the SV40 large T antigen) all kindly donated by Prof Ben-Yehuda (Hadassah Medical Organization, Israel); JJN3 (a MM cell line) kindly donated by Dr Katia Beider (Hebrew University, Israel); HEK293 (a human embryonic kidney cell line) kindly donated by Prof Ariella Oppenheim (Hebrew University, Israel); normal human fibroblasts, kindly donated by Dr Scibienski (Stockholm University, Sweden); and HC92 (a rat cardiomyocyte cell line) kindly donated by Prof Ronen Beni (Hebrew University, Israel).

Foreskin fibroblasts, HC92, HEK293 and 293T cells were grown and maintained in Dulbecco modified Eagle medium (Thermo Fisher, USA) while the other cell lines were grown and maintained in Roswell Park Memorial Institute medium (Thermo Fisher, USA). All media were supplemented with 10% fetal calf serum (Thermo Fisher, USA), L-glutamine (29.2 µg/mL), and penicillin (1,000 U/mL)/streptomycin (10 mg/mL) (Biological Industries, Israel) and incubated at 37°C in 5% CO₂. All cell lines were passaged bi-weekly and tested for mycoplasma.

Generation of cell lines expressing light chains of myeloma and AL amyloidosis patients

In order to establish a new model to study amyloidogen-

esis and its toxic effects in living human cells we used lentiviral vectors to stably express the production of amyloidogenic LC in MM cell lines. The 600 base pair LC gene was cloned within a pCR 2.1-TOPO plasmid as previously described²² (sequence in the *Online Supplementary File*). The same 600 base pair LC sequence was generated via polymerase chain reaction from this plasmid and inserted into the multiple cloning site of the minusDsRed-GFP expressing lentivirus (kindly donated by Prof. O. Mandelboim). Thus, we generated lentivirus plasmids cloned with amyloidogenic λ LC cDNA sequences from a patient who suffered from cardiac AL [H], another LC cDNA sequence from a second patient who suffered from kidney - nephrotic AL [K] and a LC sequence from a third patient who did not have AL and was denoted non-amyloidogenic MM [M]. All plasmids contained a reporter sequence of green fluorescent protein (GFP) expression. Using 293T cells we generated infectious viral particles containing λ LC and stably transduced three MM cell lines which have the intracellular machinery not only to produce but also to secrete LC proteins. Thus, we were able to create novel MM cell lines that produce, in addition to their own MM κ LC,²³⁻²⁵ an amyloidogenic λ LC and GFP. Two separate clones of each AL LC were generated (e.g., M2.3 and M2.4, or K1.4 and K1.10, or H3.8 and H3.5) and then at least three infections of each separate clone were performed on the MM cell lines JJN3, KMS11 and NCI-H292. The number of RNA transcripts for JJN3 and three separate transfections were assessed by RNA sequencing (Figure 1A). Total λ protein in KMS11 lysate (Figure 1B) and GFP expression, determined by flow cytometry (Figure 1C), detected the presence of the LC. Six biological repeats for every LC were tested in this study. These MM cell lines all produced κ LC naturally allowing the λ LC-producing plasmid to be detected and distinguished clearly from the κ production of the cell lines themselves (Figure 1D). The proliferation rate of the three lines was between 36 and 50 h.

Additionally, we transduced non-MM cell lines (HL60, 293T, 722.221) with two clones of each AL LC [H] and [K] and MM LC [M] and two separate infections as a further control to determine intracellular toxicity of the amyloidogenic LC on non-PC lines. GFP and λ expression was assessed by flow cytometry (FACSCalibur, BD Bioscience, USA) in order to determine the efficiency of infection (Figure 1C). No decrease in viability or increase in apoptosis was found in the non-PC lines transduced with the AL and MM LC (*Online Supplementary Figure S1A, C*). However, addition of exogenous AL LC was toxic (*Online Supplementary Figure S1B*). In the majority of cases more than 95% of cells were GFP-positive (Figure 1C). Using an enzyme-linked immunosorbent assay (Bethyl, TX, USA), we were able to detect the AL LC intracellularly in both MM and non-MM cell lines (Figure 1A, B), but secreted AL and MM LC only in the MM cell lines (Figure 1D). Supernatant was

collected from transfected MM cells that secreted their LC into the medium while growing. After 5 days of growth the supernatant was collected and incubated for 48 h with MM cells, primary kidney and heart cells, 721.221 and HL60, which were then assessed for apoptosis by flow cytometry following exposure to the medium containing LC. Significant increases in apoptosis (determined by propidium iodide and annexin V staining) were detected

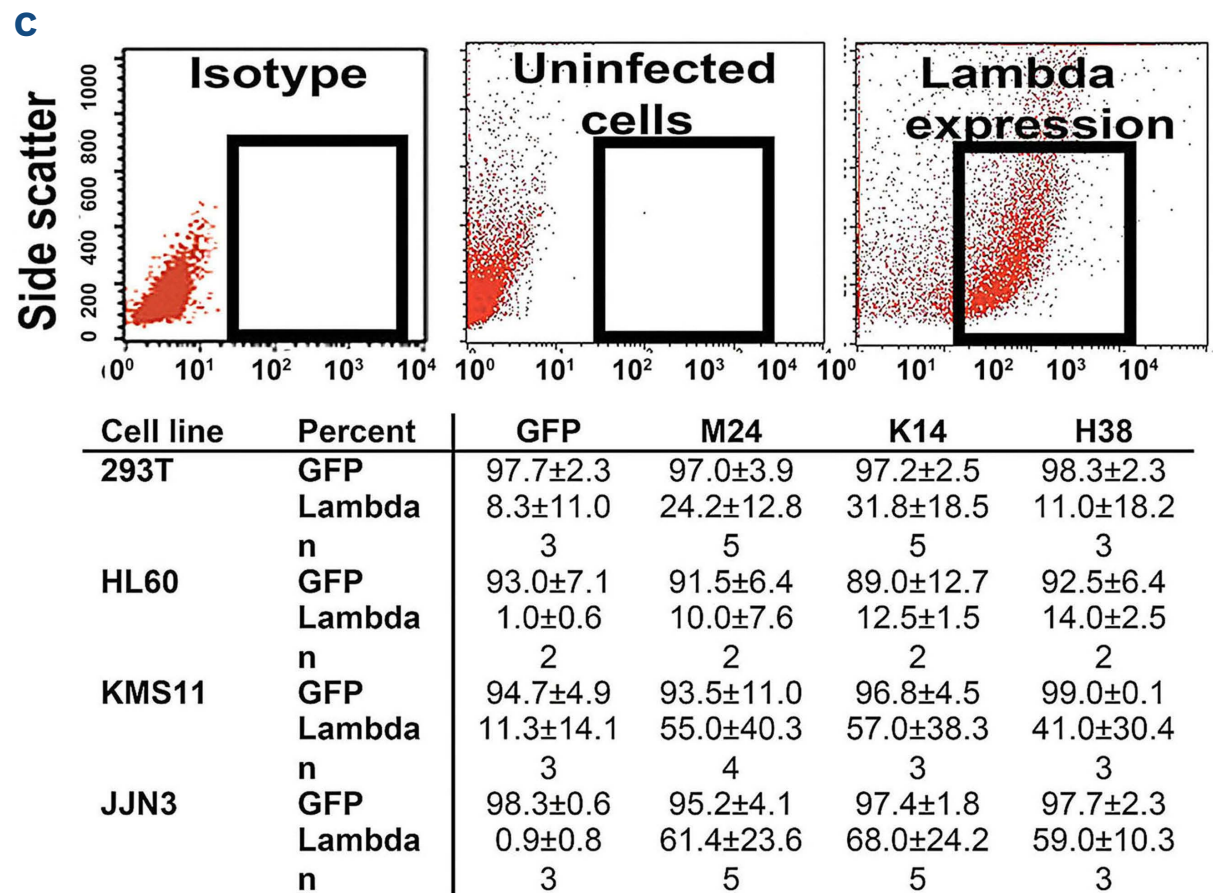
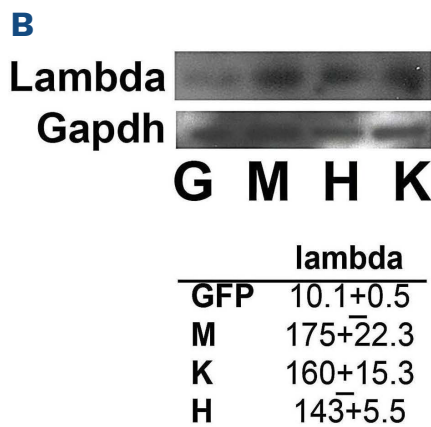
in the primary cells and MM cells when incubated with supernatant containing cardiotoxic [H] and nephrotoxic [K] LC, but not with supernatant containing non-amyloidogenic MM LC [M] (Figure 1E-G).

Cell proliferation

Ten thousand cells were seeded in wells and every 3 days a sample of cells was removed and enumerated using try-

A

JJN3	Gene Start (bp)	Gene End (bp)	M_1	M_2	M_3	K_1	K_2	K_3	H_1	H_2	H_3
	dsRed_Beg	1	2813	132	145	170	533	617	599	483	442
dsRed_End	1	2215	17291	19002	22044	133389	180755	14223	104592	104670	104601
dsRed_H	332	648	0	0	0	0	0	0	0	0	0
dsRed_H	301	331	0	0	0	0	0	0	0	0	0
dsRed_H	1	291	0	0	1	0	0	0	10260	9709	9609
dsRed_K	329	645	0	0	0	0	0	0	0	0	0
dsRed_K	298	328	0	0	0	0	0	0	0	0	0
dsRed_K	1	291	1	1	3	10816	14344	12444	0	3	2
dsRed_M	335	651	0	0	0	0	0	0	0	0	0
dsRed_M	304	334	0	0	0	0	0	0	0	0	0
dsRed_M	1	295	1747	1901	2085	10	0	0	0	0	0



D

cell line	jjn3		KMS11	721	HL60
ng/mL	Lambda	Kappa	lambda	kappa	lambda
GFP	3.7±0.1	80.0±3.3	1.2±0.5	84.2±9.2	2.2±1.5
M GFP	31.1±2.2	80.3±4.1	12.8±1.3	80.8±8.9	0.2±0.2
K GFP	26.3±3.5	83.3±7.9	11.6±1.2	75.8±7.5	5.2±0.5
H GFP	27.7±7.5	82.5±6.9	11.6±1.6	75.0±9.2	0.2±0.2

Continued on following page.

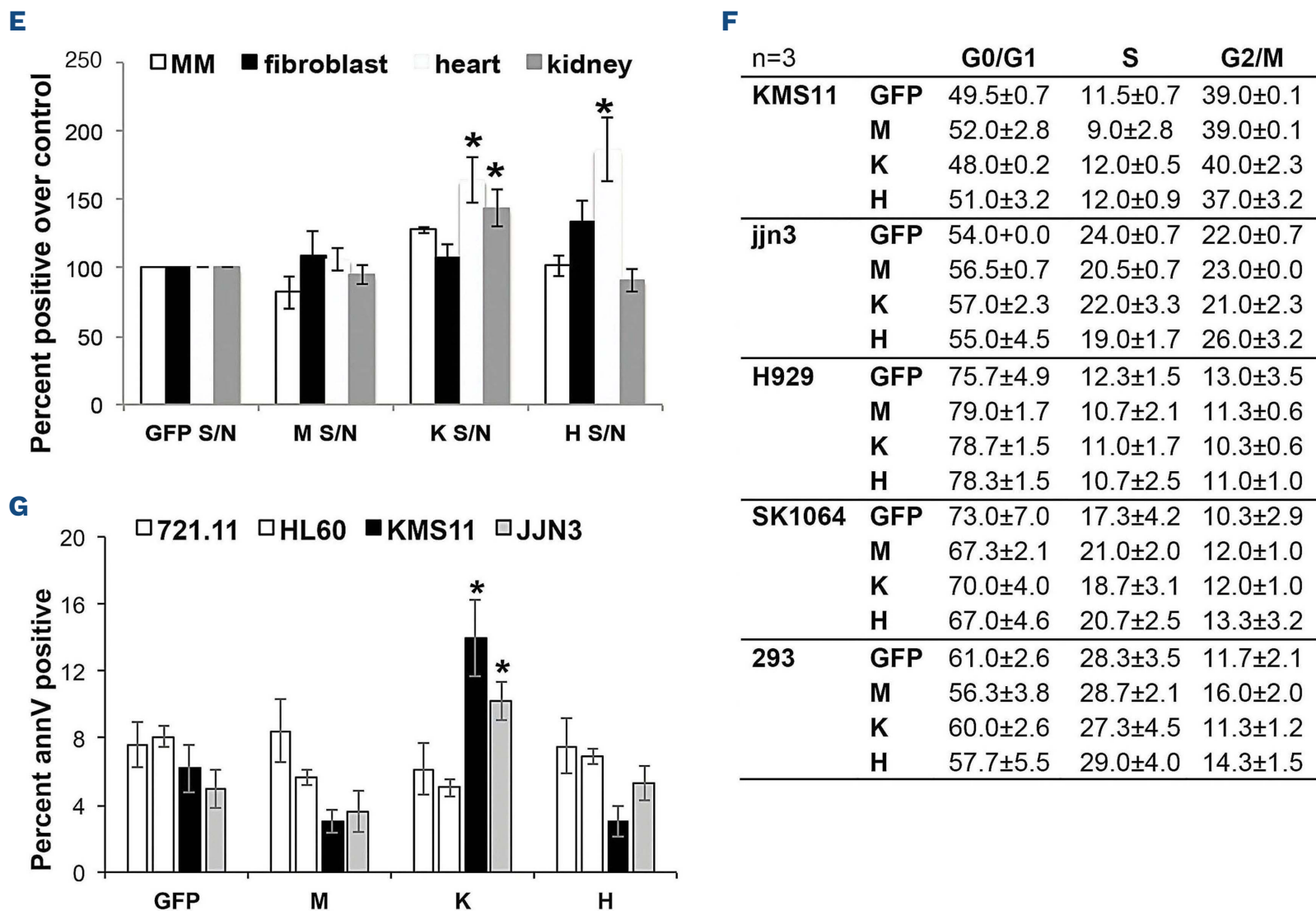


Figure 1. Assessment of intracellular and secreted λ light chains in transduced cell lines. (A) The table shows the raw counts and number of insertions, from RNA sequencing (each a separate infection of the 3 repetitions performed) of the JJN3 cell line JJN3 infected with only the green fluorescent protein (GFP) reporter or lentivirus containing cardiotoxic [H], nephrotoxic [K] amyloidogenic and multiple myeloma (MM) [M] λ light chains (LC). (B) Representative western blot illustrating the expression of λ protein in KMS11 cell lines: control (GFP [G]), AL LC ([H] and [K]), and MM LC [M] including intensity of λ bands (N=4, for separate transfections average for both JJN3 and KMS11 transduced lines). (C) Representative dot plot from flow cytometry analysis detecting monoclonal λ in the transduced KMS11 cell lines (N=6). The table shows the percent GFP and λ -positive cells from four cell lines infected (2 separate transfections). (D) Enzyme-linked immunosorbent assay to quantitate the secretion of λ LC was performed on the supernatants from which the various cell lines were grown after they had been infected. Supernatants containing secreted LC were collected 6 days after JJN3, KMS11 (MM cell lines), 721.221 and HL60 (non-MM cell lines) had been transduced with the various LC lentiviruses. GFP: empty control; [M]: multiple myeloma; [H] cardiotoxic or [K] nephrotoxic amyloidogenic LC lentivirus (N=6, 3 separate transfections in duplicate). * P <0.05 compared to GFP control. (E) Supernatants collected from MM cell lines (KMS11 and JJN3) that secreted LC and were found to contain λ LC were incubated with both MM and non-MM cell lines (JJN3, foreskin fibroblasts, heart cells [HC92] and kidney cells [HEK293]) and then the cells were assessed for increases in apoptosis (by propidium iodide staining, sub-G1 peak) as compared to the control. * P <0.05 compared to the GFP control (N=4, 2 experiments from KMS11 and 2 from JJN3 combined). (F) Cell cycle analysis of cell lines from figure (E). No significant differences in cell cycle were observed, only increases in apoptosis. (G) Supernatants that were collected from MM (JJN3) cell lines that secreted LC and were found to contain λ LC were incubated with both MM and non-MM cell lines (JJN3, KMS11, 721.221, and HL60) and cells were assessed for increases in annexin V expression as compared to control. * P <0.05 compared to the GFP control (N=4, 2 experiments from JJN3 combined).

pan blue exclusion and a hemocytometer to assess cell growth. Additionally, cell viability and proliferation were assessed using the CellTiter-Glo[®] kit (Promega, MI, USA), which measures viability and proliferation of cells by quantitating luminescence of ATP. Ten thousand cells were seeded in either quadruplicate or quintuplicate and after 5 days the proliferation was assessed by read-out of luminescence.

Cell cycle and apoptosis analysis

A re-suspended pellet of 1×10^6 cells was incubated over-

night at 4°C in 1 mL of 100% ethanol (AR. Gadot, Israel) for fixation and to minimize clumping. The cells were then washed with 1 mL phosphate-buffered saline (PBS) and treated with 50 μ L of 100 μ g/mL RNase A (Sigma-Aldrich, USA) for 30 min at 37°C to remove traces of RNA from the samples. The cells were then washed in PBS and 25 μ L of propidium iodide (1 mg/mL) were added. Samples were analyzed by flow cytometry and gated on the FL2-Width FL2-Area to identify clumps and doublets. Ten thousand events were acquired and apoptotic cells were detected in the 'SUB G1' area of the graph by a FACScalibur cyto-

meter (BD Bioscience, USA).

Annexin V binding experiments were performed using the APC Annexin V Apoptosis Detection Kit with propidium iodide (Biolegends, CA, USA). Briefly, 1×10^6 cells were washed with annexin binding buffer and then incubated with annexin V APC for 15 min at room temperature. Further washing with binding buffer was performed and 5 mL (0.5 mg/mL) of propidium iodide were added before acquisition on the FACScalibur cytometer.

Western blots

Washed and pelleted cells were lysed in cold RIPA buffer (1 mL/100 mg) containing 10 mM phenylmethylsulfonyl fluoride (Thermo Scientific), a serine protease inhibitor, and centrifuged at $\sim 14,000 \times g$ for 15 min. Supernatant was collected for western blot analysis. The samples were run in 3-(N-morpholino) propane sulfonic acid on acrylamide gels using a Sea Blue marker for size, then transferred to a polyvinylidene fluoride membrane. After transfer, the samples were blocked for 90 min with 5% skim milk solution in PBS-Tween. The membrane was incubated with primary antibody overnight at 4°C and then placed in the secondary antibody solution for 30 min. Electroluminescence was used to detect bands. The antibodies used were purchased from: Abcam (UK) – λ (1:5,000, ab109247 - polyclonal), κ – (1:20,000, ab134083 - polyclonal), c-Myc – (1:10,000, ab152146 - polyclonal), – p62 (1:1000, ab56416 - SQSTM1); Santa Cruz Biotechnology (TX, USA) – Cyclin E (1:200 of 200 mg/mL, SC-247-HE12), – GAPDH (1:400 of 200 mg/mL, SC-25778 -FL335), – Actin (1:5000, 41185 - C4) or Cell Signaling Technology (MA, USA) – Caspase-3 (1:1000, 9665-8G10), – PARP/PARP1 (1:1000, 9542).

Exogenous light chain assay

Purified LC were obtained as previously described²² from patients' 24 h urine collections. Briefly, human urine samples combined with 0.1% sodium azide (w/v) were centrifuged and ammonium sulphate was added to precipitate the LC which were then solubilized in 20 mM sodium phosphate, pH 7.0, and dialyzed against the same buffer. LC were purified by anion exchange chromatography. MM and non-MM cell lines were seeded in 96-well plates at 10,000 cells/well, in pentaplicate, and LC which were resuspended in medium were added with a pipette at the designated concentrations to medium containing cells, and cultured for 5 days. CellTiter-Glo® (Promega, USA) reagent was added and the luminescence of the plates was read using a Berthold luminometer (Titertek, Germany).

RNA extraction for RNA sequencing

We used a Qiagen RNEasy mini kit to extract RNA and tested the quality of the RNA with 6000 Nano Bio analyzer (Agilent Technologies, CA, USA). Transcriptome libraries

were prepared using the Illumina TruSeq RNA Library Preparation Kit (Illumina #RS-122-2001), according to the manufacturer's recommended protocol, starting with approximately 1.2 mg of total RNA. The amplified indexed libraries were quantified using an Invitrogen Qubit fluorometer and pooled equally according to the pool design. Pooled libraries were run on a 4% agarose gel and DNA approximately 270 base pairs long (the length of RNA inserts plus the 3' and 5' adaptors) was size-selected and recovered in 15 μ L elution buffer (QIAGEN). Size-selected libraries were then quantified again using the Qubit Fluorometer. Size was verified using High Sensitive DNA gels on an Agilent 2200 TapeStation instrument. Libraries were sequenced on a NextSeq 500 instrument using the NextSeq 500 High Output V2 Sequencing Kit (FC-404-2005), in a single-end configuration, reading 80 base pairs.

Sequencing and differential expression analysis

Raw reads were quality-trimmed at both ends, using in-house Perl scripts, with a quality threshold of 32. Following quality-trimming, adapter sequences were removed with cutadapt (version 1.9.1, <http://cutadapt.readthedocs.org/en/stable/>),²² filtering out reads that became shorter than 15 nt (-m parameter). The remaining reads were further filtered to remove very low quality reads, using the fastq_quality_filter program of the FASTX package (version 0.0.14, http://hannonlab.cshl.edu/fastx_toolkit/), with a quality threshold of 20 at 90% or more of the reads' positions.

The processed reads were aligned with up to five mismatches per read to the human transcriptome and genome using TopHat (v2.0.14).²³ The genome version was GRCh38, with annotations from Ensembl release 84. The genome was slightly modified to include the different transgenic sequences (as additional chromosomes).

Raw counts were obtained with the Cufflinks package (v2.2.1),^{24,25} using the cuffquant program with the genome bias correction (-b parameter) and the multi-mapped reads assignment algorithm (-u parameter), followed by cuffnorm. Normalization and differential expression were achieved with the DESeq2 package (version 1.12.4),²⁶ using default parameters.

Functional enrichment analysis

Downstream analysis of the expression data was done using two approaches. The first approach used a cut-off (i.e., threshold-dependent). Significantly differentially expressed genes ($P_{adj} < 0.1$) were subjected to pathway and molecular function enrichment analysis using Ingenuity Pathway Analysis (IPA®) (QIAGEN Inc., <https://digitalinsights.qiagen.com/products-overview/discovery-insights-portfolio/content-exploration-and-databases/qiagen-ipa/>). The second approach consisted of whole data analysis. Whole differential expression data from amyloidogenic

[H] and [K] versus non-amyloidogenic [M] LC-expressing cell lines were subjected to gene set enrichment analysis (GSEA).²⁶ GSEA uses all differential expression data (cut-off independent) to determine whether sets of genes, defined *a priori*, show statistically significant, concordant differences between two biological states. GSEA was run against the hallmark gene set collection from the molecular signatures database (mSigDB). Signals with normalized enrichment scores of more than 3 or less than -3 were chosen for experimental validation.

Oxidative stress measured by flow cytometry

One million cells of the JJN3 cell line and its clones were treated with either 3.3 µg/mL MitoSOX (ThermoFisher Scientific, USA) or 5 µM dihydroethidium (DHE, Sigma, USA) for 30 min in phenol-free medium. Tetramethylrhodamine methylester perchlorate (TMRM, Molecular Probes, USA) was added to the cell culture (25 nM final concentration) for the last hour of incubation. Following all incubations, cells were washed twice with PBS and then 50,000 cells were acquired and analyzed using a FACScalibur cytometer. MitoSOX measures mitochondrial superoxide while DHE measures total cellular reactive oxygen species. TMRM measures mitochondrial membrane potential.

Cholesterol assay

The Amplex[®] Red Cholesterol Assay Kit (ThermoFisher Scientific, USA) measures the concentration of both free cholesterol and cholesteryl esters by a coupled enzyme assay, which results in a colorimetric (570 nm)/fluorometric ($\lambda_{ex}=535/\lambda_{em}=587$ nm) product, proportional to the cholesterol present. The assay was performed according to the kit's instructions. MM cells from [K], [H] and [M] lines were seeded at 2×10^6 cells/50 mL of reaction mixture and assayed for free and total cholesterol levels.

Cytometric bead assay

The BD[™] Cytometric Bead Array (BD Bioscience, USA) is a flow cytometry application that allows quantification of multiple cytokines simultaneously. The Cytometric Bead Array system was used to capture cytokines secreted into the supernatant by MM cells, seeded at 1×10^5 /mL, which had been transfected with [K], [H] and [M] LC. The assay was performed according to the kit's instructions. Events were acquired on a FACScalibur and analyzed with Simplify Analysis with FCAP Array v3.0 software and Excel.

Statistics

A standard *t* test was used to determine statistically significant differences in all experiments not involving RNA assessment and RNA sequencing.

Results

Amyloidogenic light chains are toxic to plasma cells

Amyloidogenic and non-amyloidogenic MM cell lines were produced from constructs encoding cDNA from 600 patient-specific base pair-sequenced LC that were generated from patients suffering from cardiotoxic [H] and nephrotoxic [K] AL and non-amyloidogenic MM ([M]). LC sequences (*Online Supplementary Data File*) and functional changes in PC biology and growth were assessed. Multiple transfections were performed from two clones of each LC: [K], [H], and [M]. As an added control, we transduced the MM cell line with a lentiviral vector encoding only GFP [G].

We found that the MM cells (JJN3, KMS11 and NCIH929) which contained cardiotoxic [H] LC and/or nephrotoxic [K] LC had a significantly lower proliferation rate (Figure 2A, *data not shown*) and significantly more apoptosis/autophagy (Figure 2B-D, *data not shown*) than the control cell lines ([M] and [G]). The MM cells transduced with nephrotoxic [K] LC had significantly more cells in G₀/G₁ of the cell cycle and expressed higher levels of the autophagic protein p62 (Figure 2B, E) compared to control cell lines. We assessed the expression of autophagic protein p62 to determine concordance with previously published data. However, the levels of proteins involved in the cell cycle, such as Cyclin E, a protein required for the transition of cells from G₁ to S, showed no significant differences between the cell lines (*Online Supplementary Figure S2A*). Nevertheless, the levels of proteins involved in apoptosis, such as cleaved caspase 3, were increased in the MM cell lines transduced with constructs encoding amyloid LC (*Online Supplementary Figure S2A*) and these cells showed significantly lower viability, as measured by lower ATP consumption using the CellTiter-Glo[®] assay (Figure 2D and F, asterisks). Moreover, poly (ADP-ribose) polymerase (PARP), a family of proteins involved in a number of cellular processes such as DNA repair, genomic stability, and programmed cell death, was shown to be highly increased in the MM cells transduced with [K] LC (*Online Supplementary Figure S2B, C*).

To understand the selective mechanism involved in the cell proliferation and death of the cells transduced with amyloidogenic LC, RNA-sequencing analysis was performed on the cells to compare the biological effects of AL LC versus MM LC in MM cell lines. RNA-sequencing analysis of genes involved in autophagy and the intrinsic and extrinsic apoptotic pathways generated heatmaps displaying significant changes in RNA levels when the three cell lines were compared (*Online Supplementary Figure S2D*), showing that the cell lines containing AL LC had increases in death pathways in line with increases in autophagic protein p62 and apoptosis (Figure 2). FAS ligand RNA levels were upregulated in the JJN3 cell lines

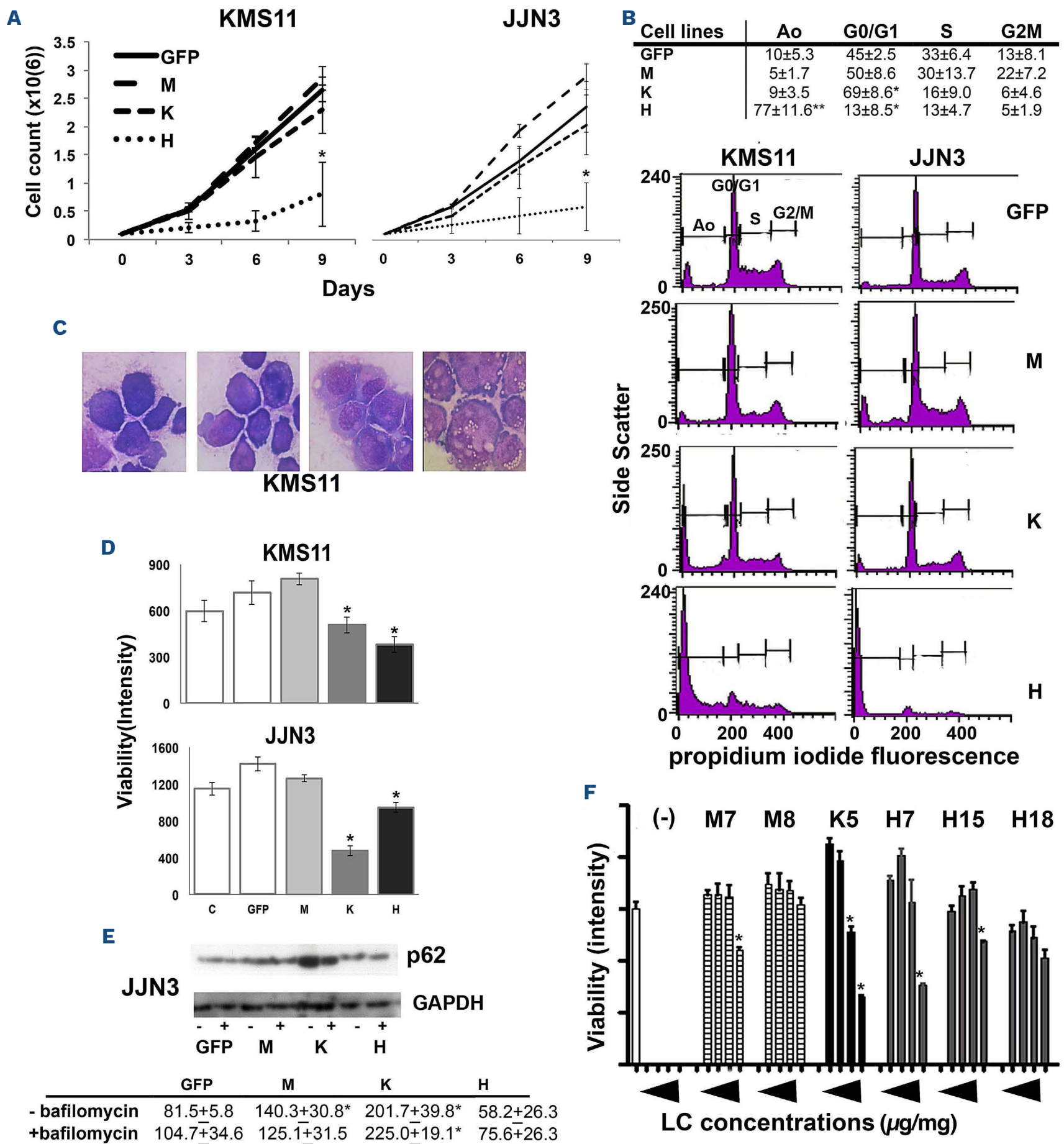


Figure 2. Cardiotoxic and, nephrotoxic amyloidogenic light chains are toxic to multiple myeloma cell lines. (A) Cell counts of multiple myeloma (MM) cell lines (JJN3 and KMS11) over 9 days following transduction with MM [M], cardiotoxic [H] or nephrotoxic [K] amyloidosis (AL) light chain (LC) constructs or with only the green fluorescent protein (GFP) reporter (5 separate infections for each cell line). (B) Cell cycle analysis of transduced MM cell lines (KMS11 and JJN3) with the previous four lentivirus constructs. Table of summary of percent cells in each stage of the cell cycle. * $P < 0.05$, ** $P < 0.01$ ($N = 6$; separate transfections 3 times JJN3 and 3 times KMS11). (C) Representative May-Grünwald staining of the MM cell line KMS11: untreated, infected with empty control lentivirus (GFP), with MM or with cardiotoxic (AL) LC ($N = 4$ separate transfections). (D) Assessment of ATP uptake (intensity) as an indicator of viability of MM cell lines (JJN3 and KMS11) that were uninfected (control, C) or infected with the same lentiviral vectors (3 separate transfections for each MM cell line). (E) Representative western blot analysis of JJN3 lysate of p62 (an autophagy substrate that is used as a reporter of autophagy activity) with (+) and without (-) bafilomycin, a potent inhibitor of cellular autophagy (6 replicate experiments, duplicate for each MM cell line). The table shows the mean \pm standard deviation of the six replicates. (F) Purified LC were isolated from patients' urine and added to the media of growing MM JJN3 cells and viability was assessed by ATP uptake (intensity) using the CellTiter-Glo[®] assay. LC from MM patients' urine (M7 and M8), LC from patients with cardiotoxic AL (H7, H15 and H18) or LC from a patient with nephrotoxic AL (K5) were incubated for 5 days with naïve JJN3 cells. Triangles indicate increases in LC concentration, i.e., 0, 50, 100, 200 and 400 mg/mL, ($N = 3$, 4-5 replicates per experiment).

transduced with MM LC, whereas caspase-3 and -6 showed trends of RNA upregulation in the cell lines transduced with [K] and [H].

When IPA® Map Activator Prediction analysis was performed, it was found that key genes in the death receptor signaling pathway were either significantly experimentally upregulated or predicted to be upregulated, as calculated from the expression of the measured genes of this pathway by both the AL LC cell lines as compared to [M] (*Online Supplementary Figure S2E*). The involvement of the autophagic pathway in AL LC toxicity has been reported elsewhere and our results concord with these findings.²⁰ To determine whether the toxicity of the amyloidogenic LC that was seen in the MM cell lines was specific to PC only, the same lentivirus combinations were transduced multiple times into 293T (kidney), HL60 (acute myeloid leukemia) and 721.221 (B lymphocyte) cell lines. We did not observe changes in viability, measured by ATP consumption, or decreases in cell cycle when the LC were produced within the cells (S and G₂M, *Online Supplementary Figure S1A-C*).

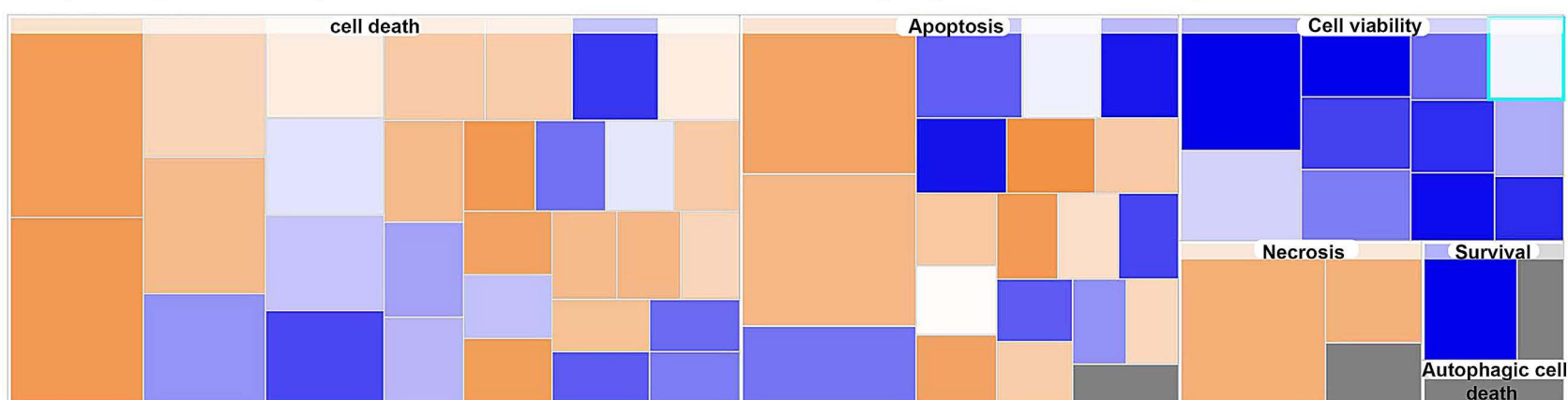
Transduced amyloidogenic light chains cause a significant increase in stress pathways in multiple myeloma cells

Further RNA-sequencing analysis was performed on the cells containing AL LC versus MM LC in order to compare biological effects in the MM cell lines. A gene expression heatmap (*Online Supplementary Figure S3A*) showed significantly upregulated or downregulated expression of various genes in the MM cells containing AL LC. An IPA®

heatmap of the cell death and survival category shows functions that are involved in cell viability and cell death for which significantly enriched differentially expressed genes were found in MM cells that contained amyloid LC ($P_{adj} < 0.1$, Benjamini-Hochberg $P < 0.05$) (*Figure 3A, Online Supplementary Table S1*). Furthermore, it is interesting to note that functions that are involved in cell death and apoptosis are predicted to be significantly upregulated, while those that are involved in cell viability are predicted to be downregulated, as reflected by IPA® z-scores that are higher than 2 in the former and lower than -2 in the latter. These results validate the phenotypic results shown earlier (*Figure 2*).

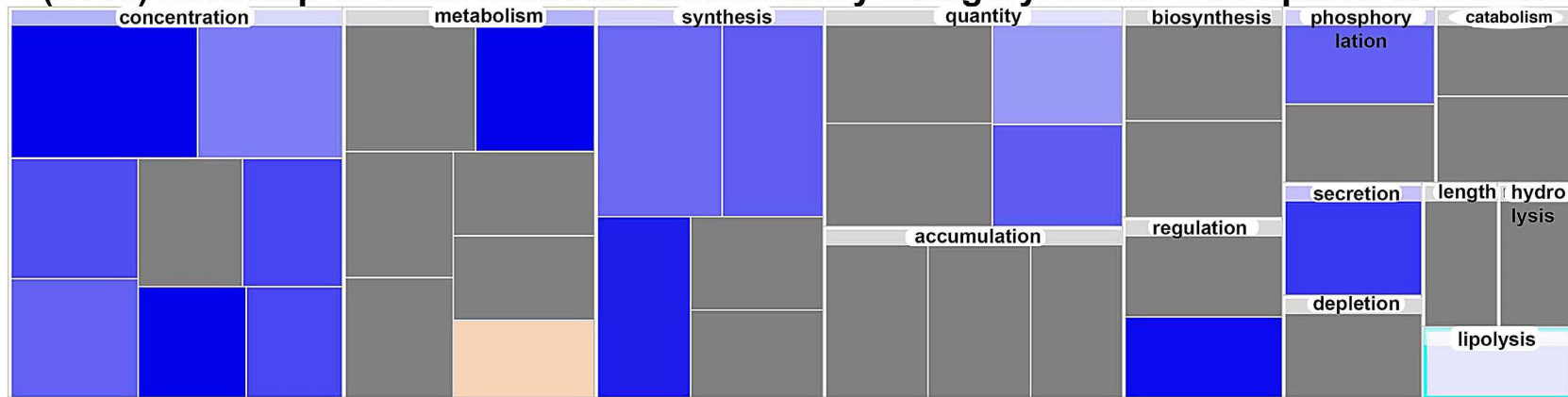
In the IPA® heatmap representing small molecule biochemistry, three molecular pathways, ‘concentration of ATP’, ‘metabolism of cholesterol’ and ‘concentration of D-glucose’, are predicted to decrease significantly in the AL LC-containing cell lines (*Figure 3B, Online Supplementary Table S2*) as compared to MM LC-containing cell lines. Interestingly, 11 significantly differentiated upregulated genes which participate in the oxidative phosphorylation enriched canonical pathway (Benjamini-Hochberg, $P < 0.05$) are upregulated in MM LC-containing cells as compared to the cell lines expressing AL LC (*Figure 4A, depicted with pink outline, Online Supplementary Table S3*). However, IPA® does not predict activation states of pathways and therefore the upregulation of these 12 genes does not necessarily signify activation of the pathway. We therefore validated this pathway *in vitro*. Mitochondrial superoxide was measured by flow cytometry in MM cell lines containing AL LC and MM LC. Similarly to data generated by sec-

A (IPA®) Heat Map of Cell death and Survival Category: K and H compared to M in JJN3 cells



Diseases or Functions Annotation	P	Predicted Activation State	Activation z-score	# Molecules
cell viability	4.57E-06	Decreased	-3.254	120
cell survival	0.0000346	Decreased	-3.162	122
cell viability of tumor cell lines	0.000248	Decreased	-2.952	73
apoptosis of bone cancer cell lines	0.00105	Increased	2.39	17
cell death of bone cancer cell lines	0.00202	Increased	2.108	19
apoptosis of leukemia cell lines	0.00357	Increased	2.034	26
cell death	2.91E-10	Increased	2.106	290

Continued on following page.

B (IPA®) Heat Map of Small Molecule Biochemistry Category: K and H compared to M in JJN3 cells

Diseases or Functions Annotation	<i>P</i>	Predicted Activation State	Activation z-score	# Molecules
concentration of ATP	0.0000407	Decreased	-2.319	18
metabolism of cholesterol	0.00124	Decreased	-2.188	13
concentration of D-glucose	0.00417	Decreased	-2.062	30

Sorted by: $-\log(P \text{ value})$ colored by: z-score

Figure 3. RNA-sequencing analysis demonstrates a significant increase in apoptotic and cell death pathways in JJN3 cells infected with amyloidogenic light chains. (A, B) QIAGEN Ingenuity Pathway Analysis® (IPA®) biological function or disease heatmap of the categories cell death and survival (A) and small molecule biochemistry (B). Each box represents a specific biological function or disease that is connected to the two functional categories above. The size of the box correlates with the gene enrichment and the color of the box indicates the predicted increase (orange, positive z-score) or decrease (blue, negative z-score). Gray indicates no change in the biological process/disease activity. Functions with IPA® z-scores >2 or <-2 are predicted to be significantly upregulated/downregulated, respectively. IPA® calculates the *P* value and the activation z-score independently and, therefore, functions with moderate enrichment can have a significant activation z-score due to hallmark genes that contribute highly to the activation state. Thirty-seven molecular functions and diseases passed the absolute z-score of 2, of which ten are shown in the tables. For all experiments, three separate transductions in JJN3 cells, $P < 0.05$.

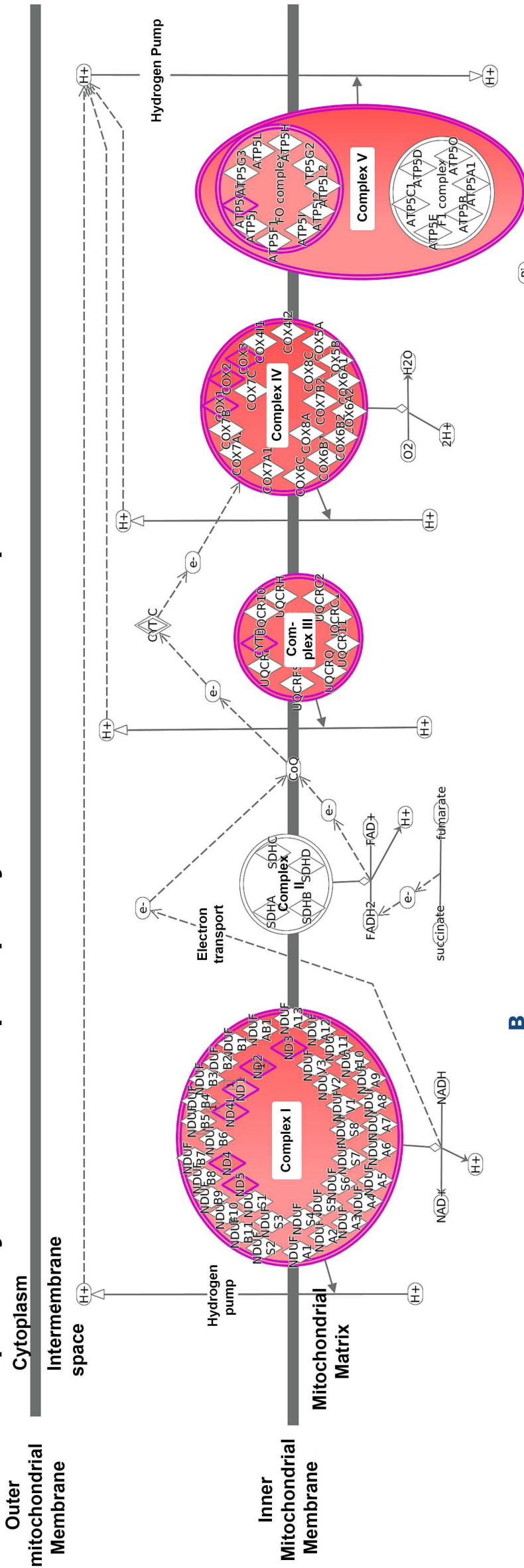
ondary RNA sequencing (Figure 4A), cells expressing AL LC ([H] and [K]) had significantly increased mitochondrial oxidative stress compared to MM cells containing non-amyloidogenic LC [M] (Figure 4B). No change was observed in mitochondrial membrane potential, as analyzed by TMRM.

Another well-established method to identify classes of genes whose expression is significantly altered between different states is GSEA. We used GSEA to compare the significant changes in gene set expression from JJN3 MM cells lines that expressed AL LC ([K] and [H]) *versus* cell lines that contained non-AL MM LC. The analysis found four gene sets with significant differences between the states. Cholesterol homeostasis, TNF α signaling via NF κ B and hypoxia were significantly enriched in the downregulated genes, while the Myc-target gene set was significantly enriched in the upregulated genes in AL LC ([H] and [K]) cells compared to non-amyloidogenic LC [M] (Figure 5A-C). Cholesterol homeostasis was significantly downregulated in the AL LC JJN3 MM cells and significantly higher levels of both free and total cholesterol were found in the cells transduced with AL LC ([H] and [K]) (Figure 5A). This result indicates a decrease in cholesterol metabolism and homeostasis, confirming the results seen in GSEA. Genes known to be Myc targets or involved in the Myc pathway were shown to be upregulated in the AL LC

MM cells and higher levels of Myc protein and RNA itself were found in these cells (Figure 5B, *Online Supplementary Figure S3B*).

TNF α enhances cell invasion via the NF κ B pathway and NF κ B controls DNA replication, cytokine production and cell survival. Genes involved in TNF α signaling via NF κ B were downregulated in the AL LC cells as compared to JJN3 MM LC cells, indicating decreased cell survival and cytokine production of the inflammatory pathway (Figure 5C, *Online Supplementary Table S4*). Secretion of various cytokines involved in the NF κ B pathway was measured in the supernatant of AL LC *versus* JJN3 MM LC cells using the the Cytometric Bead Array kit. Six cytokine levels were measured simultaneously (IL-8, IL-1 β , IL-6, IL-10, TNF α and IL-12p70). Concentrations of IL-1 β , TNF α and IL-12p70 were below the detectable limit of the assay. However, for IL-10, an anti-inflammatory cytokine, concentrations were significantly increased in AL [H] LC cells as compared to MM LC cells. In contrast, levels of the pro-inflammatory cytokines IL-8 and IL-6 were significantly lower in the AL LC-containing cells ($P < 0.02-0.0002$) (Figure 5C). It is worth noting that IL-6 is known to be involved in MM disease progression. These results indicate that the AL LC MM cells have decreased NF κ B activity, which could explain the decrease in cell viability, with the interplay balanced between various inflammatory mediators as well.

A Canonical pathway of Oxidative phosphorylation: K and H compared to M in JJJN3 cells



B Oxidative stress measured by flow cytometry in JJJN3 cells

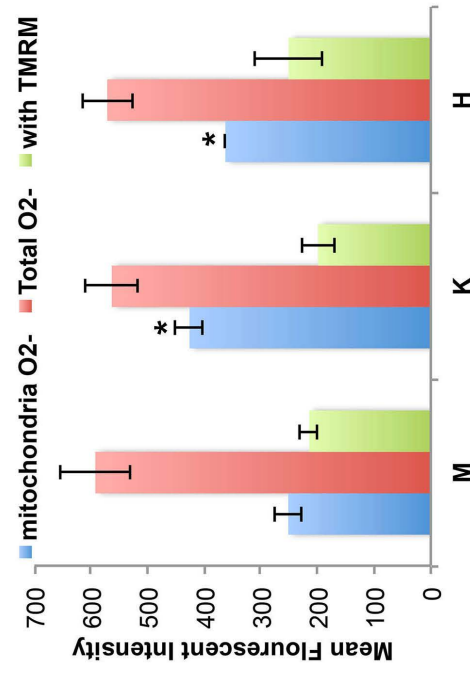
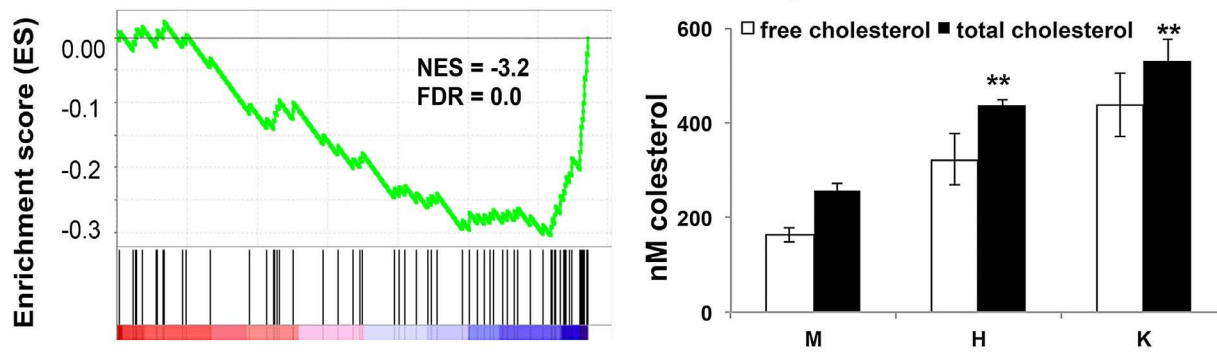
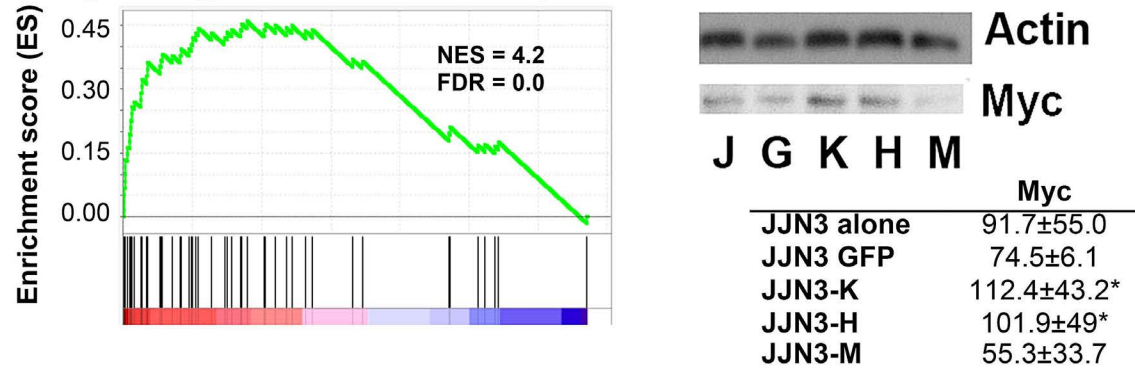


Figure 4. RNA-sequencing analysis demonstrates a significant increase in the oxidative stress pathway in JJJN3 cells infected with amyloidogenic light chains. (A) In-genuity Pathway Analysis® enriched canonical pathway for oxidative phosphorylation (Benjamini-Hochberg procedure, $P=0.046$) with pink lines showing upregulation of significantly changed genes that participate in this pathway. (B) Validation using fluorescence of reactive oxygen species, measured by flow cytometry. Multiple myeloma (MM) cells containing amyloidogenic light chains ([H] and [K]) have increased mitochondrial oxidative stress as compared to MM cells containing non-amyloidogenic light chains [M]. For all experiments, three separate transductions in JJJN3 cells, * $P<0.05$. TMRM: tetramethylrhodamine methyl ester perchlorate.

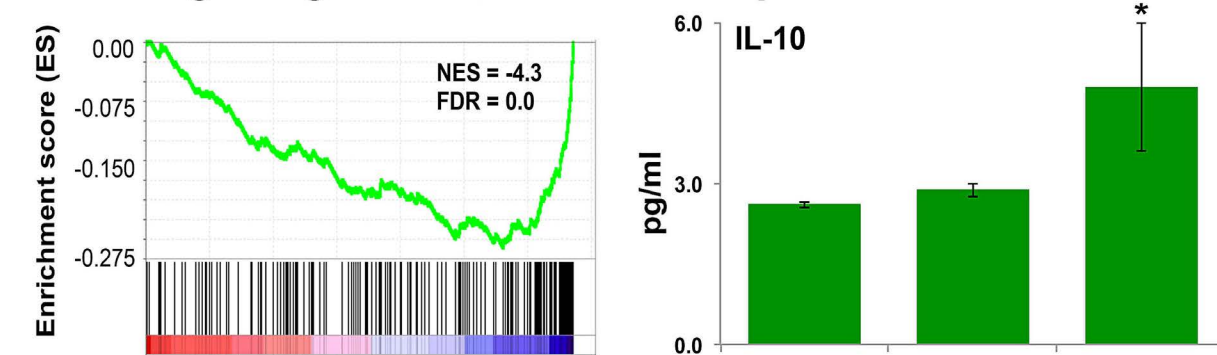
A Cholesterol Homeostasis: K and H compared to M JJN3 cells



B Myc Targets: K and H compared to M JJN3



C TNFα signaling via NFκB: K and H compared to M JJN3 cells



D Hypoxia K and H Vs M JJN3 cells

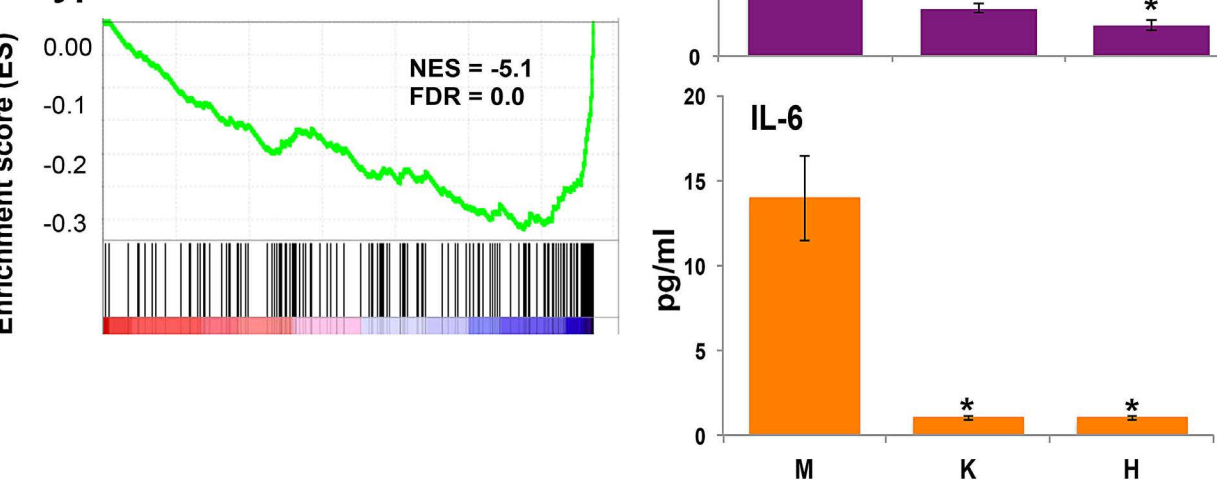


Figure 5. Gene set enrichment analysis of JJN3 cells infected with amyloidogenic versus non-amyloidogenic light chains. In the gene set enrichment analysis (GSEA), pathways represented had a normalized enrichment score (NES) of more than 3 or less than -3 and a false discovery rate (FDR) of 0.02. (A) GSEA graph of the cholesterol pathway (left) with validation using an enzyme-linked immunosorbent assay (right) to detect the presence of cholesterol in JJN3 cells expressing either amyloidogenic (AL) or multiple myeloma (MM) light chains (LC). Note the significantly higher levels of both free and total cholesterol in the cells transduced with AL LC ([H] and [K]) as compared to cells transduced with MM LC [M], N= 5, *P<0.005, **P<0.002. (B) GSEA graph of the Myc target pathway (left) and representative western blot analysis showing high levels of Myc in the cells transduced with AL LC ([K] and [H]) as compared to cells transduced with MM [M] or GFP alone [G] or untreated MM cells [J] (right). Values below are the intensities of the bands. (C) GSEA graph of TNFα signaling via NFκB (left) and concentrations of the cytokines IL-10, IL-8 and IL-6, as determined by Cytometric Bead Assay (right). Note the significant decreases of IL-8 and IL-6 in the cells transduced with AL LC ([K] and [H]) *P<0.02-0.0002. (D) GSEA graph of the hypoxia pathway. For all experiments, three separate transfections in JJN3 cells.

Finally, the gene set associated with hypoxia was found to be significantly downregulated in the AL LC MM cells (Figure 5D). Hypoxia occurs when cells are deprived of adequate levels of oxygen. If the AL LC cells are continuously

hypoxic this could contribute to the increased cell death observed in these cells. This effect may be due to the increase in reactive oxygen species causing activation of the hypoxia genes as a secondary stress response.

Discussion

The amyloid PC clone shows a selective high sensitivity to proteasome inhibitor-based therapy, resulting in a high rate of rapid, complete responses.²⁷ In previous studies this exquisite sensitivity was attributed to the oxidative endoplasmic reticulum stress induced by amyloid LC.^{20,21} Furthermore, the time to next therapy was reported to be ≥ 7 years in 60% of patients achieving complete remission after bortezomib-based therapy,²⁷ indicating a low proliferative rate of the amyloid clone, as also documented by early studies analyzing the PC labeling index.²⁸ However, the molecular basis of the indolence of the amyloid clone remained undetermined. We hypothesized that the clone size and malignant behavior may be partially influenced by the internal LC proteotoxicity to the diseased PC itself. The amyloidogenic PC in our study were phenotypically different with significant growth arrest compared to their non-amyloidogenic controls (Figure 2). Not only were they less proliferative but, additionally, the cell lines containing AL LC had higher apoptosis and autophagy (Figure 2, *Online Supplementary Figure S2*) which is compatible with the findings of previous studies.^{22,29,30} This apoptotic phenomenon was also shown to be a major mechanism of sensitivity to bortezomib in AL cells²⁰ and altering LC balance within the cells may affect AL PC survival.³¹ In this study, we demonstrate that this sensitivity was a specific internal PC effect and it did not occur in other types of non-PC lines producing AL LC.

To further delineate the underlying mechanism of the LC toxicity we subjected the transduced cells to RNA-sequencing analysis. This first revealed that the cells containing AL LC had decreased viability and increased apoptosis (Figure 3, *Online Supplementary Tables S1-3*, *Online Supplementary Figure S3B*), which could be due to major pathways involved in the metabolic stability of these cells. Pathways whose genes were significantly changed included the cholesterol pathway, Myc pathway, NF κ B signaling, hypoxia and oxidative stress (Figures 3-5). We validated the RNA-sequencing results by measuring the activation of these pathways *in vitro* and indeed found these to be more active in MM cells transduced with MM LC than in cells transduced with AL LC (Figures 3-5). This is in line with previous studies showing pro-apoptotic cascades and high oxidative stress caused by amyloido-

genic LC.^{20,30,32} RNA levels of key regulators of apoptosis and control of proliferation were found to be significantly increased during the RNA-sequencing analysis. The most significant pathways were validated herein, but many others were not investigated further in this study. Our future plans are to confirm some of these gene functions and effects of exogenous compounds in our novel model in order to delineate even more precisely the significant differences in function between a LC generated by PC from MM *versus* AL patients, and the amyloidogenic PC phenotype.

Here we have shown that a novel model of MM cells expressing AL LC *in vitro* simulated toxicity in PC and that this toxicity leads to increased apoptosis and decreased proliferation due to the malfunction of key biological processes, thus supporting our hypothesis that the AL clone size and low-grade malignant behavior may be partially influenced by internal LC proteotoxicity to the diseased PC itself. Our novel transduction system may enable future *in vitro* studies to delineate detailed AL-unique cellular pathways and devise specific targeted treatments for AL amyloidosis.

Disclosures

No conflicts of interest to disclose.

Contributions

EL, RH, JB, PR, and MP conducted experiments and analyzed the data. MP, SE, HB, YN, GM, and MEG designed the research and analyzed data. MP and MEG wrote the paper. All authors have read and revised the manuscript.

Acknowledgments

The authors thank Dr. Riki Perlman for editing the final version of the article.

Funding

This work was supported by project grants from the Israel Cancer Association, Bertha Bekhor, Hematology Research Project, Pfizer Global Medical Grant and the Adele and David Brown bequest fund in the name of the Fineberg family

Data-sharing statement

All raw RNA-sequencing data can be found online.

References

- Merlini G, Bellotti V. Molecular mechanisms of amyloidosis. *N Engl J Med.* 2003;349(6):583-596.
- Obici L, Perfetti V, Palladini G, et al. Clinical aspects of systemic amyloid diseases. *Biochim Biophys Acta.* 2005;1753(1):11-22.
- Desikan KR, Dhodapkar MV, Hough A, et al. Incidence and impact of light chain associated (AL) amyloidosis on the prognosis of patients with multiple myeloma treated with autologous transplantation. *Leuk Lymphoma.* 1997;27(3-4):315-319.
- Madan S, Dispenzieri A, Lacy MQ, et al. Clinical features and treatment response of light chain (AL) amyloidosis diagnosed in patients with previous diagnosis of multiple myeloma. *Mayo*

- Clin Proc. 2010;85(3):232-238.
5. Rajkumar SV, Gertz MA, Kyle RA. Primary systemic amyloidosis with delayed progression to multiple myeloma. *Cancer*. 1998;82(8):1501-1505.
 6. Rajkumar SV, Gertz MA, Kyle RA. Prognosis of patients with primary systemic amyloidosis who present with dominant neuropathy. *Am J Med*. 1998;104(3):232-237.
 7. Merlini G, Stone MJ. Dangerous small B-cell clones. *Blood*. 2006;108(8):2520-2530.
 8. Gatt ME, Palladini G. Light chain amyloidosis 2012: a new era. *Br J Haematol*. 2013;160(5):582-598.
 9. Palladini G, Merlini G. Current treatment of AL amyloidosis. *Haematologica*. 2009;94(8):1044-1048.
 10. Palladini G, Campana C, Klersy C, et al. Serum N-terminal pro-brain natriuretic peptide is a sensitive marker of myocardial dysfunction in AL amyloidosis. *Circulation*. 2003;107(19):2440-2445.
 11. Palladini G, Lavatelli F, Russo P, et al. Circulating amyloidogenic free light chains and serum N-terminal natriuretic peptide type B decrease simultaneously in association with improvement of survival in AL. *Blood*. 2006;107(10):3854-2858.
 12. Merlini G, Westermarck P. The systemic amyloidoses: clearer understanding of the molecular mechanisms offers hope for more effective therapies. *J Intern Med*. 2004;255(2):159-178.
 13. Phipps JE, Kestler DP, Foster JS, et al. Inhibition of pathologic immunoglobulin-free light chain production by small interfering RNA molecules. *Exp Hematol*. 2010;38(11):1006-1013.
 14. Bellotti V, Chiti F. Amyloidogenesis in its biological environment: challenging a fundamental issue in protein misfolding diseases. *Curr Opin Struct Biol*. 2008;18(6):771-779.
 15. Baden EM, Sikkink LA, Ramirez-Alvarado M. Light chain amyloidosis - current findings and future prospects. *Curr Protein Pept Sci*. 2009;10(5):500-508.
 16. Arendt BK, Ramirez-Alvarado M, Sikkink LA, et al. Biologic and genetic characterization of the novel amyloidogenic lambda light chain-secreting human cell lines, ALMC-1 and ALMC-2. *Blood*. 2008;112(5):1931-1941.
 17. Rossi A, Voigtlaender M, Janjetovic S, et al. Mutational landscape reflects the biological continuum of plasma cell dyscrasias. *Blood Cancer J*. 2017;7(2):e537.
 18. Huang XF, Jian S, Lu JL, et al. Genomic profiling in amyloid light-chain amyloidosis reveals mutation profiles associated with overall survival. *Amyloid*. 2020;27(1):36-44.
 19. Bochtler T, Merz M, Hielscher T, et al. Cytogenetic intraclonal heterogeneity of plasma cell dyscrasia in AL amyloidosis as compared with multiple myeloma. *Blood Adv*. 2018;2(20):2607-2618.
 20. Oliva L, Orfanelli U, Resnati M, et al. The amyloidogenic light chain is a stressor that sensitizes plasma cells to proteasome inhibitor toxicity. *Blood*. 2017;129(15):2132-2142.
 21. Bender S, Ayala MV, Bonaud A, et al. Immunoglobulin light-chain toxicity in a mouse model of monoclonal immunoglobulin light-chain deposition disease. *Blood*. 2020;136(14):1645-1656.
 22. Diomedede L, Rognoni P, Lavatelli F, et al. A *Caenorhabditis elegans*-based assay recognizes immunoglobulin light chains causing heart amyloidosis. *Blood*. 2014;123(23):3543-3552.
 23. Gatt ME, Takada K, Mani M, et al. TRIM13 (RFP2) downregulation decreases tumour cell growth in multiple myeloma through inhibition of NF kappa B pathway and proteasome activity. *Br J Haematol*. 2013;162(2):210-220.
 24. Dutta-Simmons J, Zhang Y, Gorgun G, et al. Aurora kinase A is a target of Wnt/beta-catenin involved in multiple myeloma disease progression. *Blood*. 2009;114(13):2699-2708.
 25. Mani M, Carrasco DE, Zhang Y, et al. BCL9 promotes tumor progression by conferring enhanced proliferative, metastatic, and angiogenic properties to cancer cells. *Cancer Res*. 2009;69(19):7577-7586.
 26. Subramanian A, Tamayo P, Mootha VK, et al. Gene set enrichment analysis: a knowledge-based approach for interpreting genome-wide expression profiles. *Proc Natl Acad Sci U S A*. 2005;102(43):15545-15550.
 27. Manwani R, Cohen O, Sharpley F, et al. A prospective observational study of 915 patients with systemic AL amyloidosis treated with upfront bortezomib. *Blood*. 2019;134(25):2271-2280.
 28. Gertz MA, Kyle RA, Greipp PR. The plasma cell labeling index: a valuable tool in primary systemic amyloidosis. *Blood*. 1989;74(3):1108-1111.
 29. Witzig TE, Timm M, Larson D, et al. Measurement of apoptosis and proliferation of bone marrow plasma cells in patients with plasma cell proliferative disorders. *Br J Haematol*. 1999;104(1):131-137.
 30. Diomedede L, Rognoni P, Lavatelli F, et al. Investigating heart-specific toxicity of amyloidogenic immunoglobulin light chains: a lesson from *C. elegans*. *Worm*. 2014;3(3):e965590.
 31. Zhou P, Ma X, Iyer L, et al. One siRNA pool targeting the lambda constant region stops lambda light-chain production and causes terminal endoplasmic reticulum stress. *Blood*. 2014;123(22):3440-3451.
 32. Mishra S, Joshi S, Ward JE, et al. Zebrafish model of amyloid light chain cardiotoxicity: regeneration versus degeneration. *Am J Physiol Heart Circ Physiol*. 2019;316(5):H1158-H1166.